Agriculture, Ecosystems and Environment 128 (2008) 1–11

Contents lists available at ScienceDirect

Agriculture, Ecosystems and Environment

journal homepage: www.elsevier.com/locate/agee

Regional carbon stocks and dynamics in native woody shrub communities of Senegal's Peanut Basin

A. Lufafa [a], J. Bolte [b], D. Wright [c], M. Khouma [d], I. Diedhiou [e], R.P. Dick [f], F. Kizito [a], E. Dossa [a], J.S. Noller [a,*]

[a] Crop and Soil Science Department, Oregon State University, Corvallis, OR 97331, USA
[b] Department of Bioengineering, Oregon State University, Corvallis, OR 97331, USA
[c] Department of Geosciences, Oregon State University, Corvallis, OR 97331, USA
[d] Laboratoire National de Recherches sur les Productions Végétales (LNRPV), Institut Sénégalais de Recherches Agricoles (ISRA), B.P. 3120 Dakar, Sénégal
[e] Institut Sénégalais de Recherches Agricoles (ISRA), B.P. 53 Bambey, Sénégal
[f] School of Natural Resources, Ohio State University, 2021 Coffey Road, Columbus, OH 43210, USA

ARTICLE INFO

Article history:
Received 14 December 2007
Received in revised form 18 April 2008
Accepted 22 April 2008
Available online 12 June 2008

Keywords:
Sahel
Agroforestry
Carbon sequestration
CENTURY model
Soil carbon management

ABSTRACT

Estimating regional carbon (C) stocks and understanding their dynamics is crucial, both from the perspective of sustainable landscape management and global change feedback. This study combines remote sensing techniques and a coupled GIS-CENTURY model to estimate regional biomass C stocks and SOC dynamics for *Guiera senegalensis* shrub communities in Senegal's Peanut Basin. A statistical model relating field-measured shrub aboveground biomass C at training plots to satellite image-derived shrub abundances was developed and used to estimate regional biomass C across a major part of the Basin. Regional SOC dynamics were modeled by coupling the CENTURY model and GIS databases. Significant correlation ($r = 0.73$; $p = 0.05$) was observed between aboveground biomass C and satellite image-derived shrub abundance at the training plots. Aboveground biomass C stocks ranged from 0.01 to 0.45 Mg ha^{-1} with an approximate total of 247,000 Mg C for the 3060 km^2 study area. CENTURY model predictions indicate that C sequestration in these systems is contingent on long-term effectiveness of non-thermal management of shrub residue and that the actual rates depend strongly on soil type and scenarios of future land management. Compared with the traditional "pruning-burned" management practice, returning prunings for 50 years would increase soil C sequestration by 200–350% without fertilization, and increase soil C sequestration by 270–483% under a low (35 kg ha^{-1} N yr^{-1}; 20 kg ha^{-1} P yr^{-1}) fertilization regime, depending on soil type and climate conditions. These results indicate that altered land management could contribute to transforming these degraded semiarid agroecosystems from a source to a sink for atmospheric CO_2.

1. Introduction

Understanding the spatial distribution of biomass carbon and sequestration potential thereof is essential for carbon (C) trading initiatives through the Clean Development Mechanism (CDM) of the Kyoto Protocol (UNFCCC, 2004). Although current project foci under the CDM exclusively target increasing C stocks in biomass, ongoing debate on a post 2012-Kyoto Protocol climate change regime show that soil C stocks are poised to start compensating fossil CO_2 emissions (Ringius, 2004; Smith et al., 2007). Indeed, as a flexibility mechanism, the Kyoto Protocol proposes that developing nations should receive "greenhouse gas credits" for increasing soil C stocks, opening up possibilities to obtain financing to support sustainable soil resource management. Success of these developments requires reliable methods for monitoring and verification of C sequestration in biomass and soil (Lal et al., 1999; Kirschbaum et al., 2001) as well as reasonable predictions of C sequestration potential across large areas.

Vegetation and soils in arid and semiarid regions control significant proportions (~46% of global terrestrial C) of terrestrial C stocks and fluxes between the land–atmosphere interface (Verhoef et al., 1996; Lal, 2001; Lal, 2002) and it is estimated that these regions have lost two-thirds of the C in areas affected by desertification (IPCC, 1996) mainly through vegetation and soil organic matter loss. Consequently, the Intergovernmental Panel on Climate Change (IPCC) estimates that these regions could

* Corresponding author. Tel.: +1 541 737 6187; fax: +1 541 737 5725.
E-mail address: jay.noller@oregonstate.edu (J.S. Noller).

0167-8809/$ – see front matter © 2008 Elsevier B.V. All rights reserved.
doi:10.1016/j.agee.2008.04.013

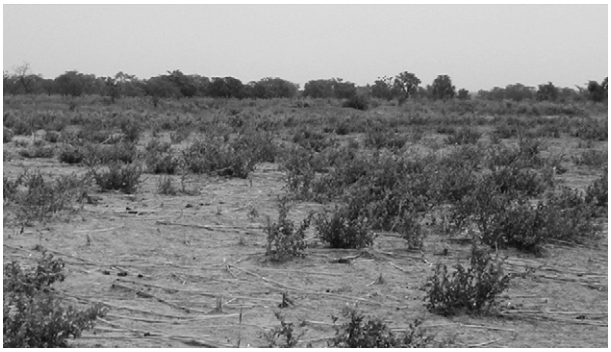

Photo 1. Field-level distribution of *G. senegalensis*.

resequester 12–19 Pg C over a 40–50-year period (IPCC, 1996) and woody shrubs are a dominant consideration for rebalancing their C budgets (Goodale and Davidson, 2002).

In Senegal and throughout neighboring Sahelian countries, there is one potentially large but poorly quantified biomass carbon pool—that of native woody shrub species (*Guiera senegalensis* J.F. Gmel) occurring in vast sections of the agricultural landscape. Our qualitative observations showed wide variations in density (average of 310 shrubs ha^{-1}) and distribution of these shrubs at both field- and landscape-level and a second-order neighborhood analysis (Lufafa et al., submitted) using Ripley's K function (Ripley, 1981) indicated these shrubs exhibit a clustered pattern (Photo 1). The shrubs are typically left to grow in farmers' fields where they are coppiced at the end of the dry season (March to April) to clear land for cultivation. Shrub stems are occasionally used for fuel and fencing homesteads while the remaining residues are burned in the field. Following the growing season, the shrubs are allowed to regrow, reaching >2 m diameters and >1 m heights. Depending on land management practices, these shrubs have the potential to be a significant source or sink for C within the global C cycle. Lufafa et al. (submitted), and Tschakert et al. (2004) quantified C stocks of these shrub systems using field assessments. While such focused individual field measurements are a step towards determining current biomass C stocks in these systems, their utility in assessing and quantifying the rather more meaningful regional scale C stock and sequestration potential (Paustian et al., 1997; Falloon et al., 2002; Ardo and Olsson, 2003) is limited because of high spatial heterogeneity and cost-related inability to have adequate sample frequency.

In this study, we estimate regional-level C stocks in *G. senegalensis* communities for a section of the Senegalese Peanut Basin using a combination of field biomass measurements and remote sensing techniques. We also couple the CENTURY model and Geographical Information System (GIS) databases to simulate current and future biomass production and soil organic carbon (SOC) in these systems under different land management practices and climate scenarios.

2. Materials and methods

2.1. Study area description

The study area is a section of the Thiés and Diourbel regions in Senegal's Peanut Basin (Fig. 1). With an areal extent of 3062 km^2, study area boundaries extend from: upper left, 276,070; 1,650,760 m and lower right 347,500; 1,590,700 m. The climate is semiarid, with a mean annual precipitation and temperature of 540 mm and 27 °C, respectively (Dacosta, 1989). Geological substrates in the area mainly include aeolian deposits of Harmattan wind sand (Herrmann, 1996) of Quaternary age over sedimentary rocks of Cretaceous to Miocene age (Monciardini, 1966), and highly eroded colluvial–alluvial ferruginous sediments derived from paleosols (Neogene) and Precambrian bedrock (Renaud, 1961; Michel, 1973). The soils classify according to Soil Taxonomy/*World Resource Base*, respectively, as: Torrox/*Ferralsols*,

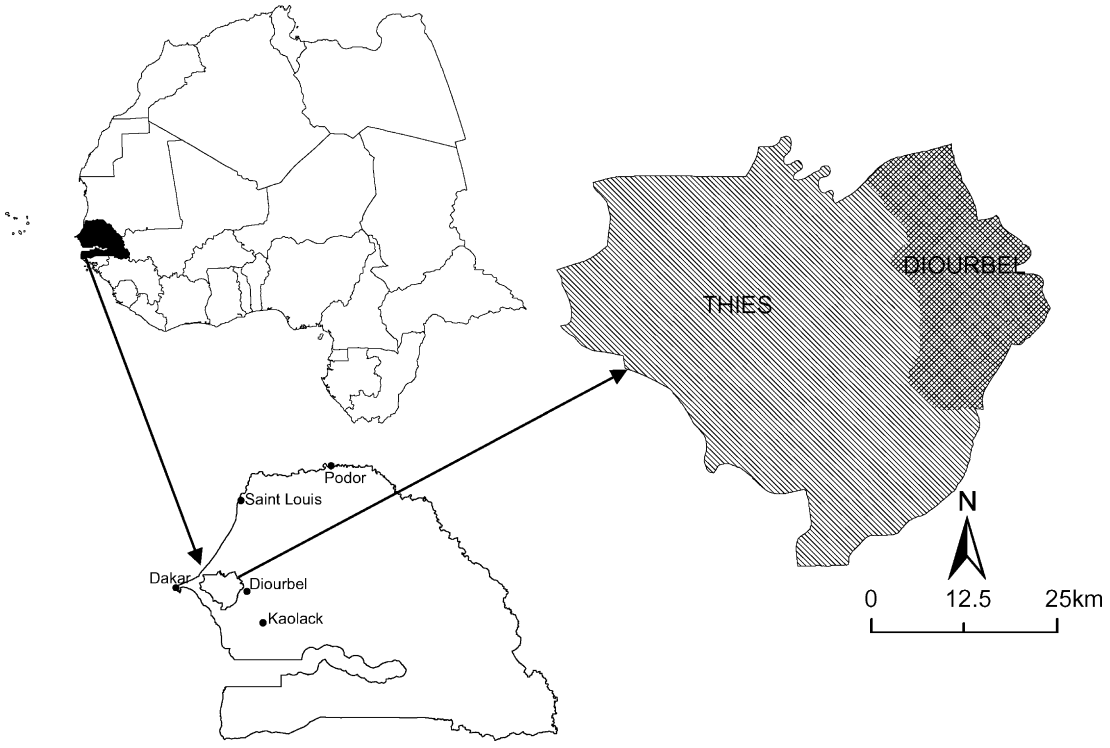

Fig. 1. Study area location.

Psamments/*Arenosols*, Torrents/*Regosols* and *Fluvisols*, Torrerts/*Vertisols*, Calcids/*Calcisols*, and Salids/*Solonchaks* (FAO, 2006). Study area vegetation is shrubland with scattered trees (Diouf and Lambin, 2001). The shrub layer is dominated by *G. senegalensis*, whereas the tree component is dominated by *Faidherbia albida*.

2.2. Regional biomass C estimation

Modules A and B in Fig. 2 jointly summarize the methods used in this study. The general approach used for estimating regional biomass C stocks (Module A in Fig. 2) is based on utilizing spectral information in satellite images for target detection and quantification (Jensen, 2000; Gonzalez and Woods, 2002). Detection of *G. senegalensis* was implemented by means of spectral unmixing or sub-pixel analysis (Elmore et al., 2000; Rosin, 2001). This approach is premised on the assumption that satellite image pixels contain materials (cover fractions) whose spectral signatures are linearly independent (and therefore linearly summed) and explain the spectral signature of a pixel as a whole (Garcia-Haro et al., 1996; Small, 2001). The cover fractions in the satellite image pixel are called endmembers (Okin et al., 1999).

Spectral unmixing decomposes satellite image pixels into constituent spectrally pure signatures of endmembers and estimates the relative combinations of the endmembers which would produce a spectral signature similar to that of the "mixed" pixel (Asner and Heidebrecht, 2002). This allows estimates to be made of the mixing proportions (or abundances) of the "mixed" pixel which is made up of the various spectral endmembers (Smith et al., 1990).

2.2.1. Selection of training plots for regional biomass C estimation

Within the study area, a georeferenced November, 1999 Landsat ETM image was used to select twenty-three 8100 m^2 (equivalent to 3×3 Landsat pixels) training plots at six sites (Table 1). The training plots were preferentially selected to maximize variability in shrub density, phenology and landscape elevation, and their size was based on the need for a uniform spatial and radiometric plot size for comparison with Landsat data and the difficulty of identifying a single Landsat pixel (30 m × 30 m) in the field without introducing spatial errors. At each site, fields with *G. senegalensis* were identified and the center coordinates of each selected field were acquired using a Garmin Etrex global positioning system (GPS). Using the center coordinates as a reference point, the nine pixels making up a 90 m × 90 m plot around the center coordinate were located on the Landsat image and the coordinates of their four outermost bounding corners recorded. Using the GPS unit, these four outermost corner points were located in the field and served as boundaries of the training plots.

2.2.2. Measurement of shrub biomass C in the training plots

Our goal was to quantify regional C stock in peak-season standing biomass of the shrubs and this occurs in late spring just before the shrubs are pruned back to prepare for the summer cropping season. Thus shrub biomass inventory for C stock estimation was done at this time of year. The procedure was to develop allometric equations that relate easily measured shrub dimensions (shrub basal and mean crown diameters) to shrub biomass (Lufafa et al. submitted). In turn, inventories of all shrubs in a given training plot in combination with the developed allometric equations (log aboveground biomass =5.12 + [0.012 × mean crown diameter]; log belowground biomass =7.52 + [0.015 × mean basal diameter]) were conducted to estimate shrub biomass. The C content of *G. senegalensis* biomass was 0.495 as determined on 24 root, stem and leaf samples using a Leco C analyzer (LECO Inc., St. Joseph, Michigan).

2.2.3. Field collection of shrub spectral signatures

To enable evaluation of the satellite image with the shrubs as endmembers, a field analysis was conducted to measure the

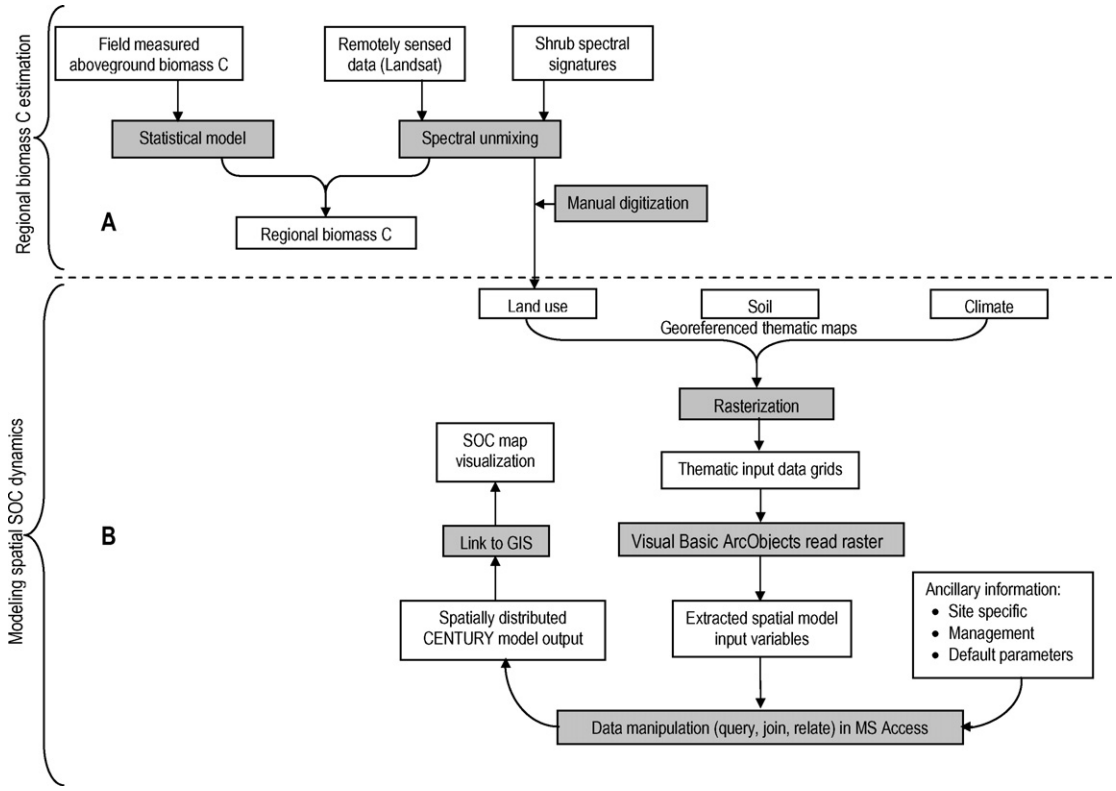

Fig. 2. Generalized methods framework for the study.

Table 1
Selected biophysical characteristics of training plots for regional biomass C estimation

Site	Plot	Soil type	Plot center coordinates		Elevation (m)	Other vegetation in plot
			Easting (m)	Northing (m)		
Keur Asanulo (n = 3)	1	Torrox	312360	1635450	103	*Acacia albida*
	2		312270	1635480	24	*Faidherbia albida*
	3		312360	1635300	29	*Acacia albida*
Keur Mandiemba (n = 4)	4		318270	1631760	25	*Balanites aegyptica*
	5		318390	1631640	47	*Balanites aegyptica*
	6		318480	1631850	23	None
	7		318180	1631430	16	None
Keur Matar Aram (n = 6)	8	Psamments	300240	1633920	87	*Acacia occidentale*
	9		300330	1633920	66	None
	10		300420	1633950	74	None
	11		300030	1633830	65	*Combretum glutinosum*
	12		299700	1633590	82	*Acacia occidentale*
	13		299610	1633500	79	None
Ndiagne (n = 2)	14	Torrox	309180	1632960	24	None
	15		309060	1632810	18	*Acacia albida*
Keur Ibra Fall (n = 5)	16	Torrents	309930	1633050	16	*Azadirachta indica*
	17		310020	1633050	16	*Combretum glutinosum*
	18		310140	1633050	24	*Balanites aegyptica*
	19		310230	1632960	25	*Acacia albida*
	20		310170	1633260	17	*Azadirachta indica*
Thilla Ounte (n = 3)	21	Torrox	318000	1636530	18	*Acacia albida*
	22		318120	1636590	27	*Acacia albida*
	23		318240	1636740	22	None

spectral properties of the shrubs in the study area. Field-based reflectance spectra of the shrub canopies were collected using a 0.35–1.050 μm (ASD, 1997) range field-portable spectrometer (FieldSPEC FR-Pro, Analytical Spectral Devices, Inc.). The instrument has a spectral resolution of approximately 3 nm at around 700 nm and measures the visible/near infrared (VNIR) portion of the spectrum using a 512-channel silicon photodiode array overlaid with an order separation filter.

Data were collected coincident with the field biomass inventories and the date of acquisition of the target Landsat image. At this time of year, the grass and most of the tree canopies were fully senescent while the shrub canopies were fully green. Spectra were consistently acquired from 0.4 to 0.5 m (nadir-looking) above the shrub canopies with a bare fiber optic having a canonical view subtending a full angle of about 25°. The spectra were then divided by the near simultaneous (<2 min) spectrum of an uncalibrated 99% reflective Spectralon panel (Labsphere, Inc.) to yield reflectance. Obtained spectra measurements of the same target were averaged to improve their signal-to-noise ratios (De Jong et al., 2003). Due to severe noise in data in the distant portions of the spectrum, only the data gathered in the 0.350 mm through 1.025 mm was used, reducing the number of spectral channels to about 470.

2.2.4. Satellite image data

A Landsat ETM$^+$ (Path 205, Row 50) image for 6th March 2004 approximately coincident with the field biomass measurement and shrub spectral signature collection campaigns was acquired and georeferenced by image to image registration on the November, 1999 image used in selecting training plots. The image was then subsetted to the extents of the study area and radiometrically normalized (Price, 1987; Markham and Barker, 1988) for factors such as sun incidence angle, time of data gathering, earth-sun distance, and sensor degradation. The radiometric data were calibrated to apparent surface reflectance in ENVI^{TM} which automatically uses the published Landsat post-launch gains and offsets (ENVI, 2004). Further corrections to the reflectance image included atmospheric normalization (Richter, 1997) using dark pixel subtraction (Elvidge et al., 1995) to remove haze (Kaufman, 1984; Du et al., 2002).

2.2.5. Spectral unmixing for pixel shrub abundance estimation

The Landsat reflectance data were spectrally unmixed to a fractional shrub abundance image using the Mixture Tuned Matched Filtering (MTMF) algorithm (Boardman et al., 1995; Funk et al., 2001) in ENVI^{TM}. MTMF is a technique designed and optimized to detect extremely weak signals that are essentially in the noise (Funk et al., 2001) and does not require knowledge of all the endmembers within an image scene. It works by separating spectral reflectance into "signal" and "noise" components. The signal is the desired spectrum scaled to represent its radiance in a pixel (Okin et al., 2001) and everything else is assumed to be noise.

First, a minimum noise fraction (MNF) was performed on the subsetted image to reduce and compress the data and to produce an image with isotropic unit variance noise that is needed in successful unmixing (ENVI, 2004). The MNF sequentially performs two cascaded principle component transformations on the data (Green et al., 1988; Boardman and Kruse, 1994): the first transformation, based on an estimated noise covariance matrix, separates white noise (i.e. uninformative data) resulting in transformed data in which the noise has a unit variance and no band-to-band correlations (Harsanyi and Chang, 1994). The second is a standard principal components transformation of the noise-whitened data and a recombination of the bands into new composite bands which account for most of the variance in the original data (Underwood et al., 2003). In the second step, the field spectral database of shrub canopies was high-frequency filtered to remove noise, resampled to Landsat wavelengths and used as the target endmember in MTMF to produce a shrub abundance image. Abundance values at known 3 × 3 pixel windows corresponding to the biomass C training plots were retrieved from the MTMF image, aggregated and used as a dependent variable in a regression against field-measured biomass C.

2.3. Modeling spatial SOC dynamics

SOC and shrub above- and belowground biomass production dynamics were simulated using Version 4 of the CENTURY model (Parton et al., 1987; Metherell et al., 1993). CENTURY is a point-based (performs simulation of and predictions for one site at a time) ecosystem model simulating biogeochemical fluxes of C, N, P, and S. To model spatial SOC dynamics across our study area, a link was made between GIS datasets and the CENTURY model (Module B in Fig. 2) by exploiting the database handling capabilities of interactive Century (i_Century). i_Century is a model control system for the CENTURY model and stores model input data in an Access database, feeds that data to CENTURY, runs CENTURY, and reads and stores the result. The basic philosophy of the i_Century approach is to manage both the input and output data of a large set of CENTURY simulations within a single database (Iowa, 2004). By handling large sample populations, i_Century provides a basis for managing spatially explicit units obtained from GIS and allows for spatially variable simulation of SOC dynamics.

2.3.1. CENTURY model default parameters

Using a combination of data from field studies, laboratory analyses and literature, we changed CENTURY default parameters to suit our study shrub species. We used a potential aboveground production of 500 g C m^{-2} yr^{-1}, altered lignin content to 14.1% and 18%, respectively for shoots and roots (Woomer et al., 2001; unpublished data), and increased the range of plant tissue C:N ratio to 50:30 in line with our laboratory analyses. Based on our field-measured biomass data and cognizant of the influence of annual pruning on biomass allocation—changing the shoot:root ratio in favor of the shoots (Brouwer, 1962; Wilson, 1988), we arrived at a fixed C allocation; about 90% of annual plant production is allocated to aboveground growth and 10% to belowground production. CENTURY is inherently a transient rather than an equilibrium model (Parton et al., 1989); so in order to bring the SOC pools of our simulated system to levels consistent with our field SOC measurements, the model was run for 1500 years using disturbance regimes obtained from anecdotal information (interviews with key informants). Due to a lack of reliable information about early system management, a generalized pattern was modified so that the 2005-year run yields a representation similar to current field observed SOC values.

2.3.2. CENTURY-GIS coupling procedure and model input parameterization

The conceptual framework for the CENTURY-GIS coupling procedure is illustrated in Fig. 2 (Module B). Land use information was derived from the satellite image through manual digitization of areas identified as having the shrubs in the MTMF image to obtain a map with two-land uses—shrubland and nonshrub land. We assumed that all shrub areas are under agricultural production with no fallows. The soil map was obtained from Centre de Suivi Ecologie (CSE) and is based on work by Stancioff et al. (1986). With a cartographic scale of 1:250,000, 12 soil unit delineations are defined according to major landscape morphological formations and topography derived from Landsat MSS data (1973–1981).

Through a combination of field measurements and literature evaluation, soil parameters needed to drive the model for the encountered soil types were obtained and georeferenced. Literature sources included: pH (Stancioff et al., 1986; Sagna-Cabral, 1989; Woomer et al., 2001), texture (Bonfils and Faure, 1956; Charreau and Vidal, 1965; Stancioff et al., 1986; Woomer et al., 2001; Elberling et al., 2003) and bulk density (Manlay et al., 2002; Tschakert et al., 2004).

Climatic data (monthly precipitation, maximum and minimum temperatures) were obtained at georeferenced climate stations from Direction de la Météorologie Nationale (DMN) in Dakar and are based on mean values during a 42-year period (1960–2002). A total of 18 climate stations (all collecting rainfall data and only four recording temperature) were used in this study.

The georeferenced soil parameter records and climate-station points were interpolated using Thiessen polygons (Mitas and Mitasova, 1999) to assign each point in space a value similar to that of the closest record. The three thematic maps (climate, soil and land use) were converted into raster at a grid resolution of 500 m corresponding to the modeling spatial scale. A point file with individual points centered in the 500 m × 500 m grid was created and a Visual Basic Arcobjects read-raster program automatically extracted the climate, soil and land use information from the thematic maps at these centered points into a table. Individual record or grid identifiers serving as the actual link between GIS and CENTURY and *X*/*Y* coordinates where added to the table using Visual Basic scripts. The obtained table was subsequently manipulated in Microsoft Access® and appended to additional information (management events, model default parameters, etc.) needed by CENTURY to produce a data structure that is compatible with i_Century. After running the model, the output was once again manipulated in Microsoft Access® to produce a table with biomass production and SOC output at desired instances for display in GIS.

2.3.3. Model simulation and scenarios

Under current management, the shrubs are pruned and the residue burned at peak-season in the spring to clear land for agricultural production. Future C stocks and sequestration potential for this "prunings burned" land management practice under contemporary and changed climate conditions were simulated by running a 2-year rotation (millet grown the first year and groundnut the second year) with grazing after each cropping season. To investigate the possibilities of increasing SOC over the period 2005–2100, we extended the simulations using hypothetical alternative management practices based on the same 2-year millet–groundnut rotation with grazing under current and future climate change scenarios. Hypothetical management included a "prunings returned" practice where the clipped aboveground biomass is chopped and returned to the soil as an amendment, a "prunings returned-low fertilization" practice where the prunings are returned and 35 kg ha^{-1} yr^{-1} N and 20 kg ha^{-1} yr^{-1} P added and a "prunings returned-high fertilization" practice with 75 kg ha^{-1} yr^{-1} N and 20 kg ha^{-1} yr^{-1} P added. Fertilization levels in the management practices are typical low- and high-end application rates for the millet crop in the study area; the contemporary climate is based on average precipitation and temperature observed from 1960 to 2002 and future climate scenarios are drawn from work on African climate change by Hulme et al. (2001) that better represents the continent's climate. Two future climate scenarios: a 1.5 °C increase in mean monthly temperature and a 25 mm decline in annual precipitation (climate change scenario 1); and a 3 °C increase in mean monthly temperature and a 50 mm reduction in annual precipitation (climate change scenario 2) were used.

3. Results and discussion

3.1. Regional biomass C stocks

Table 2 shows field-measured biomass C stock and satellite image-derived shrub abundances at the 23 training plots. There was a tenfold difference in observed aboveground C stock ranging

Table 2
Field-measured biomass C stocks and satellite image-derived shrub abundances at the training plots

Site	Plot	Biomass C (Mg)		Pixel abundance[a]
		Aboveground	Belowground	
Keur Asanulo (n = 3)	1	0.205	1.165	0.544
	2	0.143	0.825	0.381
	3	0.135	0.740	0.343
Keur Mandiemba (n = 4)	4	0.173	1.051	0.486
	5	0.123	0.714	0.330
	6	0.201	1.110	0.513
	7	0.137	0.847	0.392
Keur Matar Aram (n = 6)	8	0.284	1.617	0.748
	9	0.344	2.165	0.790
	10	0.095	0.469	0.217
	11	0.035	0.162	0.075
	12	0.276	1.391	0.643
	13	0.246	1.528	0.707
Ndiagne (n = 2)	14	0.355	1.032	0.477
	15	0.187	1.332	0.616
Keur Ibra Fall (n = 5)	16	0.345	1.098	0.508
	17	0.171	1.009	0.467
	18	0.157	0.776	0.359
	19	0.127	1.288	0.597
	20	0.149	0.826	0.382
Thilla Ounte (n = 3)	21	0.137	0.599	0.277
	22	0.122	0.828	0.383
	23	0.135	1.110	0.514

[a] Pixel abundance refers to proportion of a pixel under shrub cover. It ranges from 0 to 1, where 0 indicates shrub absence and 1 indicates total coverage of a pixel by shrubs.

from 0.035 to 0.35 Mg C with an overall mean of 0.186 Mg C (S.E.M. = ± 0.0176) and more than a tenfold difference in belowground C stock (range = 2.0; mean = 1.03; S.E.M. = ±0.087). The highest biomass C was observed at the Ndiagne site which was identified as a 2-year-old fallow while the lowest biomass was recorded at Thilla Ounte an intensively managed field. On average, there was approximately 5.8 times more biomass C in the belowground fractions as compared to the aboveground fraction (unlike belowground biomass, aboveground biomass is annually reduced by pruning) and there was a significant but rather weak correlation (belowground C = 4.4598 × aboveground $C^{0.8753}$; r = 0.87) between these two C fractions.

There is a linear and significant relationship between field-measured aboveground biomass C in the training plots and the satellite image-derived shrub abundances (Fig. 3), although considerable variability remains unexplained. The strength of this relationship progressively declined with increasing distance between training plots (unpublished data) reflecting variations in shrub spectral signature which are likely due to differences in shrub moisture content or differences in optical properties of underlying soils. The considerable amount of unexplained variability could be due to a number of reasons including the band number limitations of multispectral data, inaccuracies in georeferencing, variation in shrub spectral signature and the inherent failure of our methods to capture a more robust representation of the shrub canopies.

Propagating the statistical model (aboveground biomass C = 0.3613 × shrub abundance + 0.0175) that describes the relationship between field-measured aboveground biomass and satellite image-derived shrub through the MTMF image produced the predicted regional aboveground biomass C shown in Fig. 4. Model-predicted aboveground biomass C ranged from 0.012 to 0.45 Mg C per nine pixels (8100 m^2) with no consistent pattern or trend across the study area although there were areas of high biomass C density that were consistent with our field observations. Either our statistical model or the general method underestimates biomass C in the region because field observations show there are biomass C densities lower than 0.012 Mg and yet these are not captured in the output. This could once again be an artifact of the limitations of multispectral imagery in retrieving endmember fractions or a reflection of poor training plot selection. Although sampling plots were chosen to maximize variability, we did not sample fields with very low shrub densities and hence did not get an excellent biomass C continuum for developing the model. The failure to retrieve low biomass C abundances also could be related to limitations of the MTMF algorithm in retrieving abundances where cover of the target is less than 5% of the pixel (McGwire et al., 2000). Estimated total aboveground biomass C in the 3062 km^2 study area is 36,370 Mg and using the observed proportion of 1:5.8 for above-to-belowground biomass C, there is approximately 210,900 Mg of belowground C for a total of 247,000 Mg C in the study area at peak-season.

3.2. Biomass C production and spatial SOC dynamics

Simulation of the shrub system under contemporary climate demonstrated that total annual above and belowground shrub production ranged from 51 to 250 g C m^{-2} yr^{-1} (an artifact of differences in climate and soil type), with an average of approximately 90 g C m^{-2} yr^{-1} for the "prunings burned" management practice. The "prunings returned" practice slightly reduced average total annual shrub production by about 2.1% relative to the "prunings burned" practice and we postulate that this reflects changes in shrub-grass/crop competition mediated by fire or stimulation of relatively higher production by fire. Increased

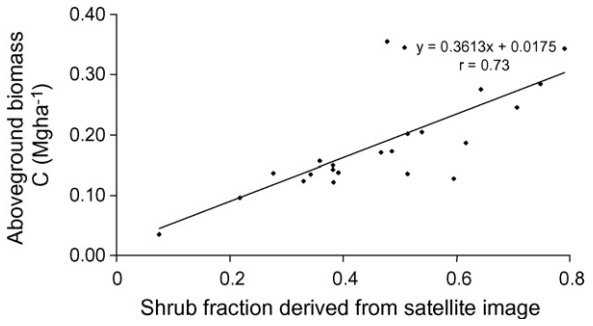

Fig. 3. Relationship between aboveground biomass C stock and shrub abundance from spectral unmixing.

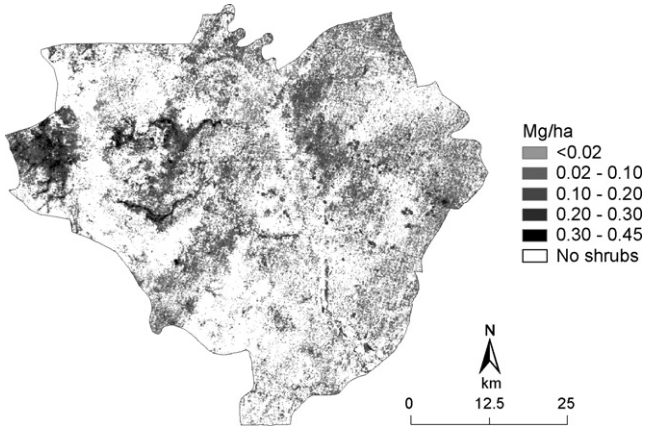

Fig. 4. Predicted aboveground biomass C stocks in the study area. Shown values have been resampled to a 90 m resolution.

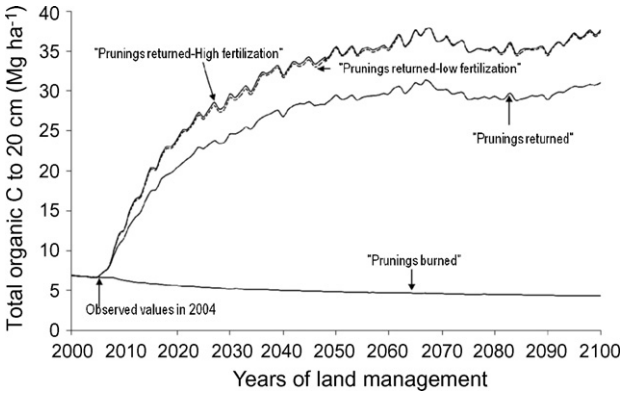

Fig. 5. Total SOC dynamics (0–20 cm depth) under the four land management scenarios.

nutrient availability through fertilization drastically improved ecosystem aboveground productivity and also increased belowground productivity to a lesser extent in both of the "prunings returned-fertilization" practices. Higher aboveground productivity (590 g C m^{-2} yr^{-1}) was predicted for the "prunings returned-high fertilization" practice at equilibrium compared to the "prunings returned-low fertilization" practice (470 g C m^{-2} yr^{-1}).

Mean SOC at equilibrium ranged from 4.9 to 35 Mg ha^{-1} depending on implemented management practice (Fig. 5). SOC of the 0–20 cm soil layer declined from 6.8 to ~4.9 Mg ha^{-1} during the 64 yrs prior to equilibrium for the "prunings burned" practice. The model-predicted dramatic changes in total SOC in the first 20 years after implementing the "prunings returned" and both of the "prunings returned-fertilization" practices and strongly suggested that significant C sequestration occurred after implementing these changes underscoring the importance of management in converting these shrub systems from CO_2 sources to sinks. These results under fertilization are contrary to Woomer et al. (2004) who proposed that C stocks could not be increased in this area through agricultural intensification because of the low rains and lack of access to irrigation.

Mean SOC at 0–20 cm increased from 6.8 to 27.2 Mg ha^{-1} for the "prunings returned" practice and from 6.8 to 33.4 Mg ha^{-1} for the two "prunings returned-fertilization" scenarios over approximately 25 yrs. Thereafter, SOC increased very slowly with average accumulation rates of 0.084 Mg ha^{-1} yr^{-1} and 0.11 Mg ha^{-1} yr^{-1}, respectively for the "prunings returned" and "prunings returned-fertilization" practices over the remaining time of the simulation. The superior sequestration potential under the "fertilization-prunings returned" practices is due to increased nutrient availability resulting from mineralization of shrub residues accompanied by increased substrate for microbial processes and the direct application of chemically recalcitrant residues (Devêvre and Horwáth, 2000).

Although the "prunings returned-high fertilization" practice produced more biomass, the resulting SOC sequestration mirrored the SOC sequestered with less biomass produced under the "prunings returned-low fertilization" practice. This indicates that beyond a certain threshold, it is not possible to increase SOC through chemical fertilizer amendments or increased biomass production. Under very fertile conditions ("prunings returned-high fertilization"), CENTURY predicts either the expression of a new hierarchical limitation (such as moisture availability) to C sequestration or an inherent insensitivity to SOC response under intense inputs. The "prunings returned-high fertilization" scenario led to superior crop yields, i.e. 2.1 and 2.5 Mg ha^{-1}, respectively, for millet and groundnut compared to 1.8 and 2.2 Mg ha^{-1} under the "prunings returned-low fertilization" practice. Economic analysis of the returns was beyond the scope of this study, but findings seem to corroborate findings by Woomer et al. (1998) who compared the C sequestration efficiency vs. the economic returns

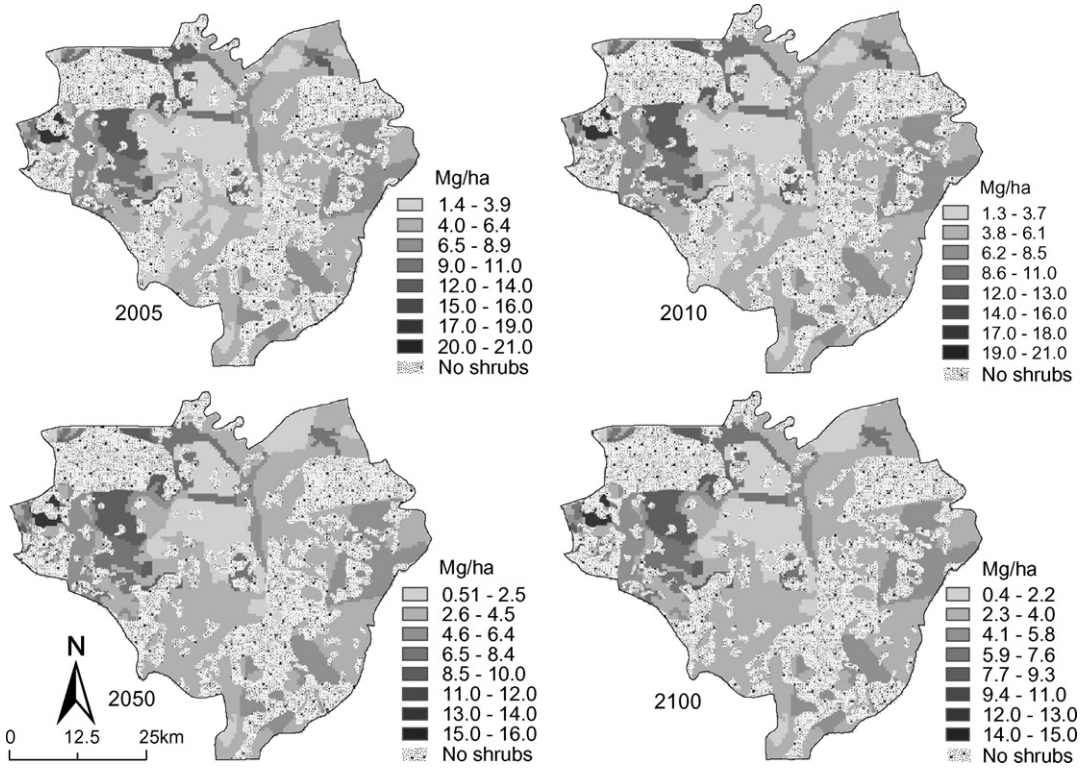

Fig. 6. Predicted SOC spatial distribution under the "prunings burned" scenario at selected time periods.

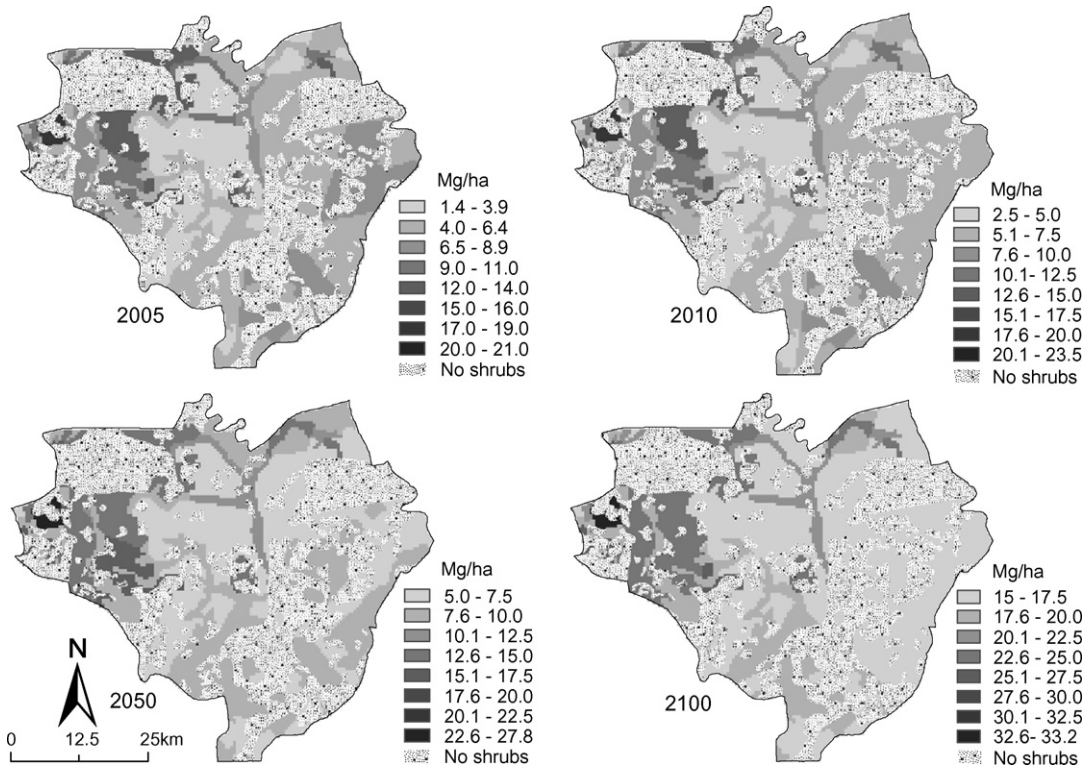

Fig. 7. Predicted SOC spatial distribution under the "prunings returned" scenario at selected time periods.

of six alternative SOC sequestration strategies in smallholdings in Kenya and showed that it was not possible to maximize both. It is also worth noting that the improved management strategies modeled here could easily conflict with farmers' major production and livelihood objectives because they involve taking economic risks to fertilize, a tradeoff between using the residues for other purposes (e.g. fuel and fencing) and also may require additional labor to manage the prunings.

Spatial distribution of simulated SOC at selected time instants for the different land management practices under the present climate is shown in Figs. 6–8. Depending on location, time to reach a steady state ranged from about 45–60 years and sequestration

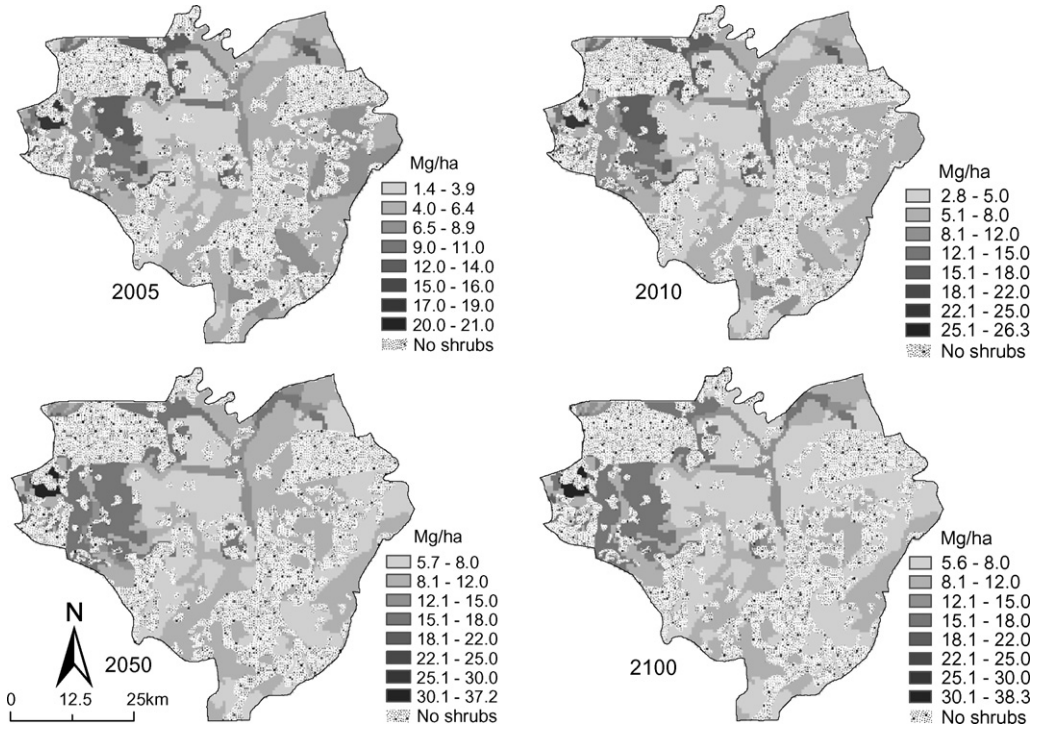

Fig. 8. Predicted SOC spatial distribution under the "prunings returned-low fertilization" scenario at selected time periods.

Table 3
Average annual SOC gains under different land management scenarios (2005–2100)

Soil type	Annual net C gain (Mg ha^{-1} yr^{-1})		
	Prunings burned	Prunings returned	Prunings returned-low fertilization
Torrerts	−0.0528	0.2270	0.2882
Torrents	−0.0368	0.1650	0.2065
Psamments	−0.0322	0.1921	0.2321
Salids	−0.0244	0.1348	0.1717
Torrox	−0.0238	0.1231	0.1557

rate ranged from 0.09 to 0.25 Mg ha^{-1} yr^{-1} for the "prunings returned" practice and from 0.09 to 0.32 Mg ha^{-1} yr^{-1} for both of the "prunings returned-fertilization" practices indicating variability in sequestration potential as a function of climate-soil type permutations. There is a north–south rainfall gradient in the area with precipitation increasing by at least 1 mm km^{-1} southwards (Camberlin and Diop, 1999). We therefore expected higher SOC values to the south as a consequence of greater plant growth (driven by precipitation) and thus superior litter inputs to soil C pools. However, equilibrium SOC values are surprisingly higher around the Thies region (northwestern part of the study area) compared to the southern parts of the area. It is highly likely that SOC in this area is more sensitive to differences in soil texture (there are heavier soils in that region) than it is to rainfall or the differences in rainfall amounts are not significant enough to elicit differences in net primary production across the study area.

Tables 3 and 4 show annual SOC accumulation rates and study area C stocks averaged by soil type, respectively. Under traditional management, the highest SOC loss rate is predicted for the Torrerts (5.28 g m^{-2} yr^{-1}) and the lowest loss rate in Torrox (2.38 g m^{-2} yr^{-1}). The fact that the soil with the lowest initial C loses the least amounts probably reflects shift towards an equilibrium at which further losses will not occur. As a proportion of 2005 stocks, the greatest SOC loss is predicted for Psamments (~38%) and the lowest loss is predicted for the Torrerts (~31%).

Model predictions indicate that if the "prunings returned" and the "prunings returned-fertilization" practices were implemented, highest absolute SOC gains are expected to occur in Torrerts (0.23 and 0.29 Mg ha^{-1} yr^{-1}, respectively for "prunings returned" and "prunings returned-fertilization") and the lowest gains are expected to occur in Torroxs (0.12 and 0.16 Mg ha^{-1} yr^{-1}, respectively for the "prunings returned" and "prunings returned-fertilization" practices). As a proportion of current C stocks, the Halosols are expected to have the highest C gains (225% and 274%, respectively for "prunings returned" and "prunings returned-fertilization" regimes, respectively) while the lowest gains are expected to occur for the Torrerts. SOC differences in the five soils indicate model sensitivity to soil texture. As expected, higher sequestration is registered in Torrerts because clay particles provide greater protection and sorption surface area for soil organic matter than do sand and silt (Amelung et al., 1998; Balesdent et al., 1998).

The improved management practices could result in the sequestration and supply of marketable C quantities, opening up possibilities for farmers in this region to obtain financing to support soil resource management. However, if carbon trading were to occur, the low sequestration rates and potential in Torrox (covering 81% of the area) will greatly reduce the amount of C credits that farmers could accumulate.

3.3. Impact of climate change on SOC sequestration

Simulated responses to changes in climate (Table 5) were complex, underscoring the potentially large impact of climate change on this ecosystem. Under the "prunings burned" practice, climate change scenario 1 reduced mean SOC by about 8% while climate change scenario 2 accentuated SOC loss by about 17%. Despite increases in temperature and reductions in rainfall, mean ecosystem SOC still increased under both climate change scenarios for the "prunings returned" and the "prunings returned-low fertilization" practices. However, relative to the baseline climate scenario, mean SOC was 21% lower under climate change scenario 1 and by 23% lower climate change scenario 2 for the "prunings

Table 4
Soil type-averaged SOC for the different land management practices at selected time periods

Soil type[a,b]	Initial SOC (Mg ha^{-1})	Mean SOC (Mg ha^{-1})								
		Prunings burned			Prunings returned			Prunings returned-low fertilization		
		2010	2050	2100	2010	2050	2100	2010	2050	2100
Torrerts (2%)	15.80	15.38	12.16	10.92	16.30	31.99	37.40	12.77	36.88	43.22
Torrents (4.2%)	10.60	10.14	7.82	7.07	11.40	23.66	26.24	12.32	27.20	30.19
Psamments (12%)	8.10	7.73	5.68	5.05	8.74	23.44	26.35	9.94	26.85	30.15
Salids (0.8%)	6.60	6.27	4.74	4.29	7.53	18.02	19.41	7.93	21.25	22.92
Torrox (81%)	6.30	5.97	4.47	4.04	6.27	16.86	17.99	6.63	19.79	21.09

[a] The average proportion (%) of sand, silt and clay is as follows for the soils: Torrerts = 44.0, 18.9, 37.1; Torrents = 88.2, 4.5, 7.3; Psamments = 48.5, 24.2, 27.3; Salids = 91.3, 4.4, 4.3; Torrox = 92.3, 3.2, 4.5.
[b] Figure in parentheses refers to percent coverage of the soil type in the study area.

Table 5
Mean study area SOC under different land management and climate scenarios

Land management scenario	Mean SOC (Mg ha^{-1})								
	Baseline climate scenario			Climate change scenario 1			Climate change scenario 2		
	2010	2050	2100	2010	2050	2100	2010	2050	2100
Prunings burned	11.20	8.47	8.30	10.47	7.78	7.49	9.52	7.03	6.72
Prunings returned	11.91	13.84	19.04	9.65	11.07	14.66	9.17	10.73	14.43
Prunings returned-low fertilization	14.98	18.97	24.90	12.28	15.37	19.42	11.76	14.61	18.92

returned" land management. For the "prunings returned-low fertilization" land management, average SOC was 19% lower under climate change scenario 1 and 23% lower under climate change scenario 2. Sensitivity analyses had shown that CENTURY was more sensitive to input temperature than input rainfall and therefore the availability of only four temperature recording climatic stations could have introduced SOC prediction errors. The lower SOC sequestration under changed climate could be due to reduced net primary productivity occasioned by a decline in precipitation and increased temperature regulation of microbial activity and mineralization of resident soil organic matter.

4. Conclusions

Reliable estimates of C stocks and dynamics in agricultural landscapes are critical to the development of practical C sequestration strategies and for development of effective policies and strategies to mitigate climate change through the CDM. Several studies measure C stocks in native shrubs of Senegal's Peanut Basin at the field level and provide important information on biogeochemical processes in this ecosystem. We demonstrate how field measurements, novel remote sensing techniques and a coupled GIS-CENTURY model can be used to estimate the more policy-relevant regional-level C estimates and dynamics in the Basin. The results indicated the following: (1) there is 247,000 Mg C at peak-season for the 3060 km^2 study area; (2) C sequestration in the native shrub systems is contingent on long-term effectiveness of non-thermal management of shrub residue; (3) altered land management could contribute to transforming these degraded semiarid agroecosystems from a source to a sink for atmospheric CO_2; (4) regardless of adapted land management practice, anticipated future climate changes will reduce SOC sequestration potential of the system. Estimates of regional C stock could be improved by using hyperspectral satellite data, using training plots that represent the entire observed continuum in shrub density while accuracy of SOC dynamics could be improved by availability of more temperature recording stations and a higher number of more evenly distributed soil parameter observations.

Acknowledgments

This research was supported by the Geoscience Biocomplexity Program of the National Science Foundation (Award 0120732). We thank Papa Serigne Sarr, Younouss Tamba, Papa Omar Dieye and Moussa Diop of ISRA for helping in data collection, Analytical Spectral Devices (ASD) for lending us the Spectroradiometer, Joan Sandeno for editing the manuscript and the anonymous reviewers for the valuable comments.

References

Amelung, W., Zech, W., Zhang, X., Follett, R.F., Tiessen, H., Knox, E., Flach, K.W., 1998. Carbon, nitrogen, and sulfur pools in particle size fractions as influenced by climate. Soil Sci. Soc. Am. J. 62, 172–181.

Ardo, J., Olsson, L., 2003. Assessment of soil organic carbon in semi-arid Sudan using GIS and the CENTURY model. J. Arid Environ. 54, 633–651.

ASD, 1997. FieldSPEC User's Guide, Manual Release. Analytical Spectral Devices, Inc. Boulder, Colorado, USA.

Asner, G.P., Heidebrecht, K.B., 2002. Spectral unmixing of vegetation, soil and dry carbon cover in arid regions: comparing multispectral and hyperspectral observations. Int. J. Remote Sens. 23, 3939–3958.

Balesdent, J., Besnard, E., Arrouays, D., Chenu, C., 1998. The dynamics of carbon in particle-size fractions of soil in a forest cultivation sequence. Plant Soil 201, 49–57.

Boardman, J.W., Kruse, F.A., 1994. Automated spectral analysis: a geological example using AVIRIS data, north Grapevine Mountains, Nevada. In: Proceedings, ERIM Tenth Thematic Conference on Geologic Remote Sensing, Environmental Research Institute of Michigan, Ann Arbor, MI, pp. 1407–1418.

Boardman, J.W., Kruse, F.A., Green, R.O., 1995. Mapping target signatures via partial unmixing of AVIRIS data. Summaries of the 5th JPL Airborne Earth Science Workshop, 95-1, 1. JPL Publication, pp. 23–26.

Bonfils, P., Faure, J., 1956. Les sols de la region de Thies: Annales du Centre de Recherches Agronomiques de Bambey au Senegal. Bull. Agronomique 16, 6–92.

Brouwer, R., 1962. Distribution of dry matter in the plant. Neth. J. Agric. Sci. 10, 399–408.

Camberlin, P., Diop, M., 1999. Inter-relationships between groundnut yield in Senegal, interannual rainfall variability and sea-surface temperatures. Theor. Appl. Climatol. 63, 163–181.

Charreau, C., Vidal, P., 1965. Influence de l'Acacia albida Del. sur le sol, la nutrition minerale et les rendements des mils Pennisetum au Senegal. L'Agronomie Tropicale 7, 601–626.

Dacosta, H., 1989. Preciptations et ecoulements sur le bassin de la Casamance, Ph.D. Thesis, University of Cheikh Anta Diop, Dakar.

De Jong, S.M., Pebesma, E.J., Lacaze, B., 2003. Above-ground biomass assessment of Mediterranean forests using airborne imaging spectrometry: the DAIS Peyne experiment. Int. J. Remote Sens. 24, 1505–1520.

Devêvre, O.C., Horwáth, W.R., 2000. Decomposition of rice straw and microbial carbon use efficiency under different soil temperatures and moistures. Soil Biol. Biochem. 32, 1773–1785.

Diouf, A., Lambin, E.F., 2001. Monitoring land-cover changes in semi-arid regions: remote sensing data and field observations in the Ferlo, Senegal. J. Arid Environ. 48, 129–148.

Du, Y., Guindon, B., Cihlar, J., 2002. Haze detection and removal in high resolution satellite image with wavelet analysis. IEEE Trans. Geo. Remote Sens. 40, 210–217.

Elberling, B., Touré, A., Rasmussen, K., 2003. Changes in soil organic matter following groundnut-millet cropping at three locations in semi-arid Senegal, West Africa. Agric. Ecosyst. Environ. 96, 37–47.

Elmore, J.E., Mustard, J.F., Manning, S.J., Lobell, D.B., 2000. Quantifying vegetation change in semi-arid environments: precision and accuracy of spectral mixture analysis and the normalized difference vegetation index. Remote Sens. Environ. 73, 87–102.

Elvidge, C.D., Yuan, D., Weerackoon, R.D., Lunetta, R.S., 1995. Relative radiometric normalization of Landsat Multispectral Scanner (MSS) data using an automatic scattergram controlled regression. Photogramm. Eng. Remote Sens. 61, 1255–1260.

ENVI, 2004. The Environment for Visualization of Images. ENVI User Guide. ENVI version 4.1. Research System Inc., 864 pp.

Falloon, P., Smith, P., Szabó, J., Pásztor, L., 2002. Comparison of approaches for estimating carbon sequestration at the regional scale. Soil Use Manage. 18, 164–174.

Funk, C.C., Theiler, J., Roberts, D.A., Borel, C.C., 2001. Clustering to improve matched filter detection of weak gas plumes in hyperspectral thermal imagery. IEEE Trans. Geo. Remote. Sens. 39, 1410–1420.

Garcia-Haro, F.J., Gilabert, M.A., Melia, J., 1996. Linear spectral mixture modeling to estimate vegetation amount from optical spectral data. Int. J. Remote Sens. 17, 3373–3400.

Gonzalez, R.C., Woods, R.E., 2002. Digital Image Processing, second ed. Prentice Hall, New Jersey.

Goodale, C.L., Davidson, E.A., 2002. Carbon cycle: uncertain sinks in the shrubs. Nature 418, 593–594.

Green, A.A., Berman, M., Switzer, P., Craig, M.D., 1988. A transformation for ordering multispectral data in terms of image quality with implications for noise removal. IEEE Trans. Geo. Remote Sens. 26, 65–74.

Harsanyi, J.C., Chang, C.I., 1994. Hyperspectral image classification and dimensionality reduction: an orthogonal subspace projection approach. IEEE Trans. Geo. Remote Sens. 32, 779–785.

Herrmann, L., 1996. Staubdeposition auf Böden West-Afrikas. Eigenschaften und Herkunftsgebiete der Stäube und ihr Einfluß auf Boden und Standortseigenschaften. Hohenheimer Bodenkundliche Hefte 36, 239.

Hulme, M., Doherty, R., Ngara, T., New, M., Lister, D., 2001. African climate change: 1900–2100. Clim. Res. 17, 145–168.

Iowa State University, 2004. i_Century, http://www.public.iastate.edu/~elvis/i_century_main.html. Iowa State University.

IPCC, 1996. Climate change 1995: the science of climate change. In: Houghton, J.T., Meira Filho, L.G., Callander, B.A., Harris, N., Kattenberg, A., Maskell, K. (Eds.), Contribution of Working Group 1 to the Second Assessment Report of the Intergovernmental Panel on Climate Change. Cambridge University Press, Cambridge.

Jensen, J.R., 2000. Remote Sensing of the Environment: An Earth Resource Perspective. Prentice Hall, Upper Saddle River, New Jersey.

Kaufman, Y.J., 1984. Atmospheric effects on remote sensing of surface reflectance. SPIE 475, 20–33.

Kirschbaum, M.U.F., Schlamadinger, B., Cannell, M.G.R., Hamburg, S.P., Karjalainen, T., Kurz, W.A., Prisley, S., Schulze, E.D., Singh, T.P., 2001. A generalized approach of accounting for biospheric carbon stock changes under the Kyoto Protocol. Environ. Sci. Pol. 4, 73–85.

Lal, R., 2001. Potential of desertification control to sequester carbon and mitigate the greenhouse effect. Clim. Chan. 51, 35–72.

Lal, R., 2002. Carbon sequestration in dryland ecosystems of west Asia and North Africa. Land Degrad. Dev. 13, 45–59.

Lal, R., Hassan, H.M., Dumanski, J., 1999. Desertification control to sequester C and mitigate the greenhouse effect. In: St. Michaels Workshop on Carbon

Sequestration and Desertification, Pacific Northwest National Lab., St. Michaels. Batelle Press, pp. 83–149.
Manlay, R.J., Kaire, M., Masse, D., Chotte, J., Ciornei, G., Floret, C., 2002. Carbon, nitrogen and phosphorus allocation in agro-ecosystems of a West African savanna. I. The plant component under semi-permanent cultivation. Agric. Ecosyst. Environ. 88, 215–232.
Markham, B.L., Barker, J.L., 1988. Radiometric properties of U.S. processed Landsat MSS data. Remote Sens. Environ. 22, 39–71.
McGwire, K., Minor, T., Fenstermaker, L., 2000. Hyperspectral mixture modeling for quantifying sparse vegetation cover in arid environments. Remote Sens. Environ. 72, 360–374.
Metherell, A.K., Harding, L.A., Cole, C.V., Parton, W.J., 1993. CENTURY soil organic matter model environment. Technical documentation. Agroecosystem Version 4.0. Great Plains System Research Unit Technical Report 4. USDA Agricultural Research Services, Fort Collins, CO.
Michel, P., 1973. Le Bassins des fleuves Senegal et Gambie: Etude geormophologique. Tomes I a III. ORSTOM 365.
Mitas, L., Mitasova, H., 1999. Spatial interpolation. In: Longley, P., Goodchild, M.F., Maguire, D.J., Rhind, D.W. (Eds.), Geographical Information Systems: Principles, Techniques, Management and Applications. GeoInformation International, Wiley, pp. 481–492.
Monciardini, C., 1966. La sedimentation eocene au Senegal. Memoir de Bureau de Recherche en Geologie et Mines No. 43.
Okin, W.J., Okin, G.S., Roberts, D.A., Murray, B., 1999. Multiple endmember spectral mixture analysis: endmember choice in an arid shrubland. Summaries of the 8th JPL Airborne Earth Science Workshop, 99-17, 1. JPL Publication, pp. 323–331.
Okin, G.S., Okin, W.J., Murray, B., Roberts, D.A., 2001. Practical limits on hyperspectral vegetation discrimination in arid and semiarid environments. Rem. Sens. Environ. 77, 212–225.
Parton, W.J., Schimel, D.S., Cole, C.V., Ojima, D.S., 1987. Analysis of factors controlling soil organic matter levels in Great Plains grasslands. Soil Sci. Soc. Am. J. 51, 1137–1179.
Parton, W.J., Cole, C.V., Stewart, J.S.B., Ojima, D.S., Schimel, D.S., 1989. Simulating regional patterns of soil C, N, and P dynamics in the U.S. Central grassland region. In: Clarholm, M., Bergstrom, L. (Eds.), Ecology of Arable Land. Kluwer Academic Publishers, pp. 99–108.
Paustian, K., Levine, E., Post, W.M., Ryzhova, I.M., 1997. The use of models to integrate information and understanding of soil C at the regional scale. Geoderma 79, 227–260.
Price, J.C., 1987. Special issue on radiometric calibration of satellite data. Remote Sens. Environ. 22, 1–158.
Renaud, L., 1961. Le precambrian du sud-ouest de la Mauritania et du Senegal Oriental. Memoir, de Bureau de Recherche en Geologie et Mines No. 5. 134 pp.
Richter, R., 1997. Correction of atmospheric and topographic effects for high spatial resolution satellite imagery. Int. J. Remote Sens. 18, 1099–1111.
Ringius, L., 2004. Soil carbon sequestration and the CDM: opportunities and challenges for Africa. Clim. Chan. 54, 471–495.
Ripley, B.D., 1981. Spatial Statistics. Wiley, New York.
Rosin, P.L., 2001. Robust pixel unmixing. IEEE Trans. Geo. Remote Sens. 39, 1978–1983.
Sagna-Cabral, M.A., 1989. Utilisation et gestion de la matiere organique d'origine animale dans un terroir du centre nord du Senegal. Memoire d'Etude, Centre National d'Etudes Agronomiques des Regions Chaudes (CNEARC), Montpellier, France.
Small, C., 2001. Estimation of urban vegetation abundance by Spectral Mixture Analysis. Int. J. Remote Sens. 22, 1305–1334.
Smith, M.O., Ustin, S.L., Adams, J.B., Gillespie, A.R., 1990. Vegetation in deserts. I. A regional measure of abundance from multispectral images. Remote Sens. Environ. 31, 1–26.
Smith, P., Martino, D., Cai, Z., Gwary, D., Janzen, H., Kumar, P., McCarl, B., Ogle, S., O'Mara, F., Rice, C., Scholes, B., Sirotenko, O., 2007. Agriculture. In: B. Metz, O.R. Davidson, P.R. Bosch, R. Dave, L.A. Meyer (Eds.), Climate Change 2007: Mitigation. Contribution of Working Group III to the Fourth Assessment Report of the Intergovernmental Panel on Climate Change, Cambridge University Press, Cambridge, United Kingdom and New York, NY, USA.
Soil Survey Staff, 2003. Soil Taxonomy, Third edition. USDA/NRCS Agriculture Handbook 436.
Stancioff, A.M., Staljanssens, M., Tappan, G., 1986. Mapping and Remote Sensing of the Resources of the Republic of Senegal: a Study of the Geology, Hydrology, Soils, Vegetation and Land Use Potential. South Dakota State University, Remote Sensing Institute, SDSU-RSI-86-01, South Dakota, USA.
Tschakert, P., Khouma, M., Sene, M., 2004. Biophysical potential for soil carbon sequestration in agricultural systems of the Old Peanut Basin of Senegal. J. Arid Environ. 59, 511–533.
Underwood, E., Ustin, S., DiPietro, D., 2003. Mapping nonnative plants using hyperspectral imagery. Remote Sens. Environ. 86, 150–161.
UNFCCC, 2004. UN Framework Convention on Climate Change, http://unfccc.int/index.html. UNFCCC.
Verhoef, A., Allen, S., De Bruin, H.A.R., Jacobs, C.M.J., Heusinkveld, B.G., 1996. Fluxes of carbon dioxide and water vapour from a Sahelian savanna. Agric. Forest Met. 80, 231–248.
Wilson, J.B., 1988. A review of the evidence on the control of shoot:root ratio in relation to models. Annals Bot. 61, 433–449.
Woomer, P.L., Palm, C.A., Qureshi, J.N., Kotto-Same, J., 1998. Carbon sequestration and organic resource management in African smallholder agriculture. In: Lal, R., Kimble, J.M., Follett, R.F., Stewart, B.A. (Eds.), Management of Carbon Sequestration in Soil. Advances in Soil Science. CRC Press Inc., Boca Raton, USA.
Woomer, P.L., Tieszen, L.T., Tschakert, P., Parton, W.J., Touré, A., 2001. Landscape Carbon Sampling and Biogeochemical Modeling: A Two-Week Skills Development Workshop Conducted in Senegal. SACRED Africa, Nairobi, Kenya.
Woomer, P.L., Touré, A., Sall, M., 2004. Carbon stocks in Senegal's Sahel transition. J. Arid Environ. 59, 499–510.
World Resource Base (WRB), 2006. World Soil Resources Reports No. 103. FAO, Rome.